A Hodgkin-Huxley model for conduction velocity in the medial giant fiber of the earthworm, *Lumbricus terrestris*

Charles Heller[1] and Kevin Crisp[1]
[1]*St. Olaf College, Northfield, Minnesota 55057*

The speed of nerve impulse conduction, or conduction velocity, is crucial to the survival of animals. For example, rapid conduction velocity in the nerve pathways underlying escape behavior represents a distinct evolutionary advantage. Peripheral demyelinating diseases can lead to a loss of conduction velocity and subsequent serious symptoms and diseases, such as the fatigue and gait deficiencies commonly observed in multiple sclerosis patients. A better understanding of the biophysical mechanisms underlying conduction velocity may yield insights that could be valuable in the development of therapies for such diseases. Nerve cord gigantism and myelin sheath are the two basic mechanisms that increase the conduction speed of electrical nerve impulses. The giant fibers of the common earthworm *Lumbricus terrestris* are made up of many neurons electrically coupled by high fidelity gap junctions, permitting a unique perspective on the contribution of transmembrane ionic currents on conduction velocity. Furthermore, the previously noted taper in diameter of the oligochaete giant fibers along the longitudinal axis presents another unique opportunity to study the role of morphological properties on conduction velocity, even within a single fiber pathway. The role of these gap junctions and their interaction with axonal taper in predicting conduction velocity has not been studied closely in the annelid. Intracellular recording from individual giant fibers in earthworm is very challenging, and the genetic and pharmacological tools are not yet available to manipulate gap junction communication reliably. Because of these technical limitations, a combination of extracellular electrophysiology, histology, and computational modeling were used to explore the influence of, and interaction between, electrical coupling and axon diameter on conduction velocity. We observed that conduction velocity in the medial giant fiber (MGF) seems to be predicted by a nonlinear supra-additive interaction between axonal conductance and gap junction conductance. This suggests that both are critical considerations when studying nerve impulse conduction.

Abbreviations: g_a – axonal conductance, g_c – gap junction conductance, H-H – Hodgkin and Huxley, LGF – Lateral Giant Fiber, MGF – Medial Giant Fiber

Keywords: computational model; cuticle; gap junction

Introduction

The common earthworm (*Lumbricus terrestris)* ventral nerve cord contains a medial giant fiber (MGF) that runs from anterior to posterior of the worm, and bilateral giant fibers (LGFs) that run posterior to anterior. The MGF is composed of a chain of approximately 100 interneurons. Each of these neurons is electrically connected to its neighbors in the next-most rostral and next-most caudal body segments (Lyckman and Bittner, 1992 and Zoran and Martinez, 2009). The same is true of each LGF. The two LGFs are fused together via frequent interconnects and thus are considered one functional giant axon (Bullock, 1945; Guenther, 1973; Zoran and

Martinez, 2009). It has been shown in the related species *Lumbriculus variegatus*, that both the MGF and LGF show a distinct taper in axon diameter. The LGF increases in diameter from anterior to posterior and the MGF decreases (Zoran and Drewes, 1987; Zoran and Martinez, 2009). Cable theory, our basis for understanding the electrophysiological properties of nerve impulse conduction, predicts that these anatomical features will cause a change in conduction velocity as nerve impulses propagate longitudinally along the giant fibers (Kandel, 2005). In this paper, we investigate this hypothesis in the MGF of the common earthworm, *Lumbricus terrestris.*

In order to understand the background for this hypothesis, it is helpful first to consider the evolution of nerve gigantism in species such as the earthworm. As the diameter of an axon increases, so too does the conduction velocity in that axon. This can be understood by considering the equivalent circuit model of a passive axon. Due to the absence of active ion channels, the anatomical properties and their impact on conduction are highlighted by this model. This commonly used approach to computational modeling (Friesen and Friesen, 1994) represents ionic conductances as resistors and the axon membrane as a capacitor. In this way, basic electronic theory can be used to explain various physiological phenomena (such as charging time of the membrane). Of the parameters in this model, the inner longitudinal resistance (R_l), outer longitudinal resistance ($R_{e)}$, and membrane capacitance C_m are the most important in determining the speed of electrical conduction (Hartline and Coleman, 2007). Namely, the product: (R_l + R_e)C_m, must be small for rapid conduction velocity (Hartline and Coleman, 2007).

In this model, membrane C_m and R_l are the two parameters that depend on axon diameter. Capacitance at any point along the axon varies directly with the circumference of the axonal cross section. Because circumference is equal to πd, the relationship between diameter and capacitance is linear, or first-order. Longitudinal resistance, however, is inversely related to the cross sectional area of the axon. Because cross sectional area is equal to the area of a circle, $A = \pi(\frac{d}{2})^2$, the relationship between diameter and R_l is of second-order. Thus, for an increase in axon diameter, R_l decreases faster than C_m increases, and the overall product (R_l + R_e)C_m decreases. Evidence to support this concept is easily observed by comparing the speed of conduction velocity in the smaller diameter LGF, which has a slower conduction velocity than the larger diameter MGF (Bullock, 1945; aGuenther, 1973; Drewes et al., 1978).

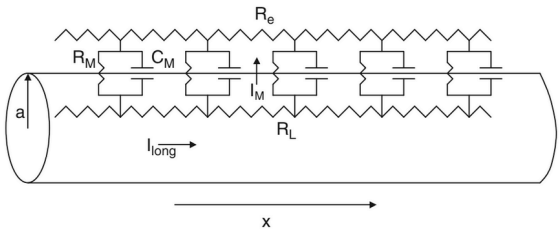

Figure 1: Equivalent circuit model of the passive axon. R_M represents the membrane resistance, C_M the capacitance, R_L the interior longitudinal or axonal resistance, R_e the exterior longitudinal resistance. I_M and I_{long} represent membrane and axon ion currents, respectively.

The equivalent circuit model for nerve axons in Figure 1 is a simplified view of the worm giant fibers. In order to create a physiologically accurate model of the nerve axon, one must consider the variable membrane resistance of the phospholipid bilayer to different ions due to the opening and closing of individual ion channels. Through their study of the squid giant axon, Hodgkin and Huxley created a model that achieves this (Hodgkin and Huxley, 1952). Their model includes the specific membrane

conductances for Na^+ and K^+ ion channels and an overall leak channel conductance, as well as a reversal potential for each ion (Figure 2).

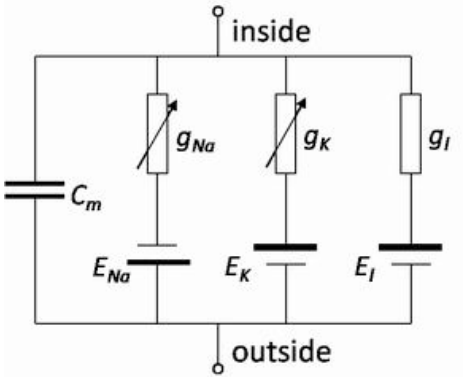

Figure 2: Hodgkin-Huxley equivalent circuit model of the squid giant axon. The two variable resistors, g_{Na} and g_K, represent voltage dependent Na^+ and K^+ conductance, the fixed resistor, g_l, represents a voltage independent leakage conductance. C_m represents the membrane capacitance, and E_{Na}, E_K, and E_l are the reversal potentials for Na^+, K^+, and leakage potentials, respectively.

Using a system of 12 partial differential equations, Hodgkin and Huxley were able to develop a model that accurately describes the biophysical properties of an action potential in the squid giant axon (Nelson, 1966). In this paper we use a common adaptation of the H-H model to investigate the propagation of an action potential across gap junctions in the MGF of the earthworm (Friesen and Friesen, 1994). We predict that electrophysiological and histological studies will confirm the presence of axon taper and longitudinal change in conduction velocity that has been observed in *Lumbricus variegatus*. We hypothesize that computationally modelling nerve impulse conduction across gap junctions in the MGF will allow us to draw conclusions about the role gap junctions play in determining conduction velocity.

Material and Methods

An interdisciplinary approach consisting of electrophysiology, histology, and computational methods was taken. Physiological and anatomical constraints on the computational model were obtained using data from sections 1.1 and 1.2. The goal of the computational model was to test the sufficiency of the parameters g_a and g_c in explaining the observed physiological phenomenon.

1.1 Electrophysiology

Multi-unit extracellular recordings were taken from the earthworm medial giant fiber (n = 5). Four Ag/AgCl electrodes were spaced evenly along the length of each worm, each connected to an AD instruments AC/DC differential amplifier (Dunedin, New Zealand, Model 3000) as illustrated in Figure 3.

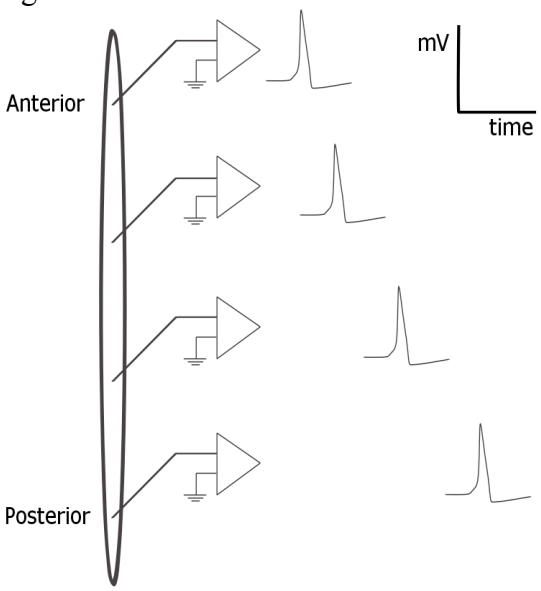

Figure 3: Illustration of setup for electro-physiological recordings of earthworm MGF. Spikes shown to the right of each recording point shown are computer generated, not from earthworm MGF. The vertical axis is voltage and the horizontal is time.

Data was acquired and digitized at 10kHz using AD instrument's PowerLab 26T (LTS) data acquisition hardware, and

spike timestamps were found using the peak detector function on LabChart software (version 8). Peak detector function worked by locating the first zero derivative following set threshold crossing. This was done independently for each channel in each recording. Animals acquired from Super America bait shop (Lakeville, MN) were anesthetized using 0.2% chloretone for 5 minutes prior to recording.

Because the skin and body muscle of these animals is thin, it is sufficient to simply insert the electrodes into the tissue and record electrical signals (Kaldt et al., 2010). In order to stimulate the medial giant fiber, a brief tap was delivered to the earthworm's cuticle using the end of a toothpick (Kaldt et al., 2010; Shannon et al., 2014). Because the MGF runs from anterior to posterior and the LGF posterior to anterior, only MGF spikes were elicited by stimulation of the cuticle. Due to the earthworm's internal segmentation, the impedance between recording sites is very high and thus each unit was well isolated. Stimulation was delivered once every minute for 5 minutes to avoid sensitization or adaptation to the stimulus. One minute intervals were chosen by experimentally determining which interval reliably induced spikes. If multiple spikes were triggered following a stimulus, all action potentials from that trial were analyzed and recorded. Mean conduction velocities between each recording location were calculated and compared. Statistical significance was tested in MATLAB (MathWorks) using custom written software for a bootstrapped distribution of means and comparing it with our results.

1.2 Histology

One earthworm was sacrificed and two 10-20 segment sections were taken from the animal and fixed in Bouin's fixative. One section came from the anterior of the animal and one from the posterior. Specimens were then moved through a series of ethanol dilutions (Table 1) and embedded in paraffin wax (60°C) in peel-away molds. Tissue was oriented so that vertical cross-sections of the animal could be obtained.

A Leica microtome was used to cut 8µm cross-sections of tissue. Tissue sections were adhered to 1:1 albumin-glycerol prepared slides and rehydrated and stained with Gomori's trichrome (reagents from Fischer Inc., Waltham, MA, unless noted) using a series of washes (Table 2). Slides were then dried thoroughly, deparaffinized, rehydrated, stained, and dehydrated a final time using a series of washes (Table 2). Sections were then covered in 3 drops of Permount and coverslipped.

Using a conventional Olympus brightfield microscope and a 40X lens, the earthworm nerve cords were imaged and the area of the MGF at each cross section was recorded. All histology procedures followed those used by Cole et al. (2011) and are detailed in the following tables.

Table 1: Dehydration procedure

Solution	Time
50% EtOH	24 hours
50% EtOH	24 hours
70% EtOH	1 hour
95% EtOH	1 hour
100% EtOH	1 hour
100% EtOH	1 hour
Toluene	1 hour
Toluene	1 hour
Paraffin-saturated Toluene	1 hour
60°C melted paraffin	1-2 hours

Table 2: Rehydration and staining procedure

Solution	Time
Toluene	6 minutes
100% EtOH	3 minutes
100% EtOH	3 minutes
95% EtOH	3 minutes
70% EtOH	3 minutes
50% EtOH	3 minutes

30% EtOH	3 minutes
DI Water	10 minutes
Gomori Trichrome Stain	45 seconds
2X rinse in DI water	10 dips each
500X glacial acetic acid	30 seconds
95% EtOH	3 minutes
95% EtOH	3 minutes
100% EtOH	3 minutes
Toluene	6 minutes

1.3 Computational modeling

Using the H-H model to simulate the spiking of a neuron, an electrical synapse of the earthworm medial giant fiber was created using python programming language (version 3.4). This model is illustrated in Figure 4.

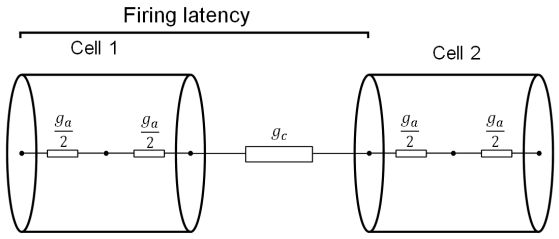

Figure 4: Illustration of computationally modeled gap junction in MGF of the earthworm. Firing latency refers to the time between spikes in cell one and cell two. Each cell is divided into two compartments, each representing half of the overall axonal conudctance, g_a.

The original parameters chosen by Hodgkin and Huxley for the reversal potential of Na^+, K^+, and leak channels were left unchanged (Hodgkin and Huxley, 1952). However, the respective conductance of each ion channel was altered to best fit the electrophysiological data. The membrane potential in each compartment was determined by the voltage in the compartment immediately preceding it and by the voltage in the compartment immediately following it, as well as by the axonal conductance, g_a, between compartments as shown in equation 1 (Friesen and Friesen, 1994).

Equation 1:

$$V = \frac{-g_{Na}(V - E_{Na}) - g_K(V - E_K) - g_l(V - E_l) + g_a(V_{prev} - V)}{C_m} dt$$

If at a gap junction, g_c was used in place of g_a (equation 2).

Equation 2:

$$V = \frac{-g_{Na}(V - E_{Na}) - g_K(V - E_K) - g_l(V - E_l) + g_a(V_{prev} - V)}{C_m} dt$$

Both g_a and C_m were made to vary with diameter as discussed in the introduction. g_c was independent of diameter. An arbitrary stimulus of ionic current was input briefly into the first compartment in order to initiate the propagation of an action potential.

In order to determine the relative contribution of g_a and g_c to conduction velocity in each case, a sensitivity analysis was conducted on the two parameters. To do this, both parameters were randomly varied for 1000 trials. Combinations of g_a and g_c that yielded firing latencies in agreement with physiological data were saved.

Data from the sensitivity analysis was output into MATLAB where it was plotted and analyzed qualitatively for which parameter, g_c or g_a, had the larger influence on determining conduction velocity. To do this, data were plotted next to a theoretical model where both parameters were weighted equally in predicting conduction velocity. This was accomplished by locating the maximum value of each parameter observed in the results of the computational model, normalizing these values to one, and plotting a line from g_a max to g_c max.

Results

1.1 Electrophysiology

MGF spikes were recorded at four points along the length of animals (n=5; Figure 5). When comparing the mean conduction velocity in anterior, middle, and posterior sections across all animals,

conduction velocity was found to be lower in the posterior of the worm compared to the anterior (Figure 5).

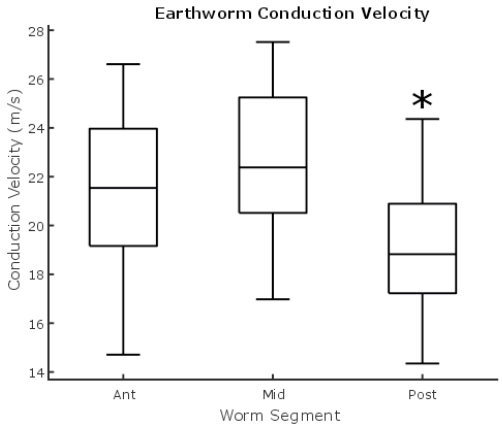

Figure 5: Conduction velocity measurements in anterior, middle, and posterior (n = 5). Anterior conduction velocity was significantly greater than the posterior conduction velocity, as was the middle conduction velocity ($p < 0.001$). Anterior and middle conduction velocity means did not significantly differ. Mean conduction velocities +/- SEMs are as follows: anterior: 21.48 +/- 0.52 m/s, middle: 22.47 +/-0.45 m/s, posterior: 19.09 +/- 0.44 m/s.

The mean conduction velocity in the posterior portion of the worm was significantly slower than the anterior ($p < 0.001$). Conduction velocity in the middle of the worm was found not to be significantly different from the anterior, but was found to be significantly greater than the posterior ($p < 0.001$). All significance was determined based on comparison of the difference in mean between two given groups with a bootstrapped distribution of differences in mean. Alpha levels were set to 0.05. Though the sample size of n = 5 is small, the results were consistent across all animals and were consistent with previous observations in other studies, namely in *Lumbriculus variegatus.*

1.2 Histology

Histological sectioning, shown in Figure 6, showed a decrease in cross sectional axon area from anterior to posterior (n = 1). Despite a sample size of one, it is reasonable to accept this difference as it agrees with previously observed axon taper in *Lumbriculus variegatus* and would also be expected given the electrophysiology results in this and previous studies. Lateral giant fibers seem to have disappeared in the anterior portion of the worm, as their axons are too small at this point (Figure 6).

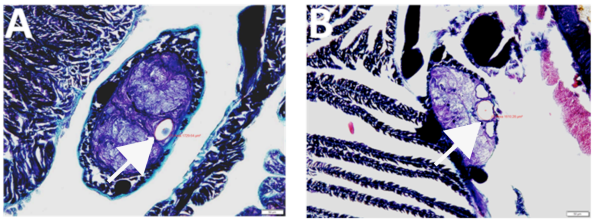

Figure 6: (A) Cross section through anterior sample of earthworm. MGF axon (arrow) cross sectional area was measured to be 1729.64 μm^2. (B) Cross section through posterior sample of earthworm. MGF axon (arrow) cross sectional area was measured to be 1610.28 μm^2. LGF axons are absent from anterior cross section.

1.3 Computational model results

Given the preceding anatomical data, as well as the knowledge that the MGF consists of electrically coupled interneurons, a model was constructed to test the sufficiency of these relationships in predicting conduction velocity. Using the physiological and anatomical constraints obtained in 1.1 and 1.2, the model indicates that at individual gap junctions along the MGF, conduction velocity is primarily explained by axonal conductance, not by the strength of electrical coupling between the two neurons. Thus, in this model conduction, velocity is more sensitive to electrical coupling, $g_{c,}$ than to axonal conductance, g_a.

In Figure 7, successful combinations of g_c and g_a for both fast and slow conduction velocities are plotted. As conduction velocity increases, solutions approach the theoretical additive line shown

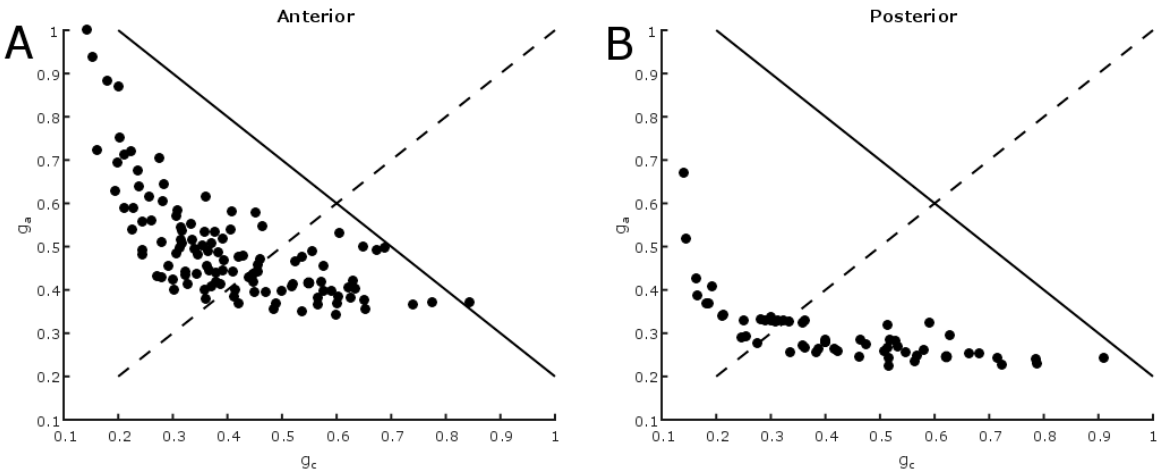

Figure 7: Supra-additive effects of g_c and g_a on conduction velocity. Successful combinations of g_a and gc are plotted above. Panel A represents results for rapid conduction velocities (anterior of the worm) and panel B represents results for low conduction velocities (posterior of the worm). The solid line represents a theoretical perfectly linear, additive model. The dashed line represents the points where g_a is equal to g_c. In a perfectly linear, additive model solutions would be expected at the intersection of these two lines. Values of g_c and g_a are normalized to the maximal conduction parameter measured in any trial.

in Figure 8. This finding is not inconsistent with a supra-additive interaction between g_a and g_c, being sufficient to explain conduction velocity in the MGF.

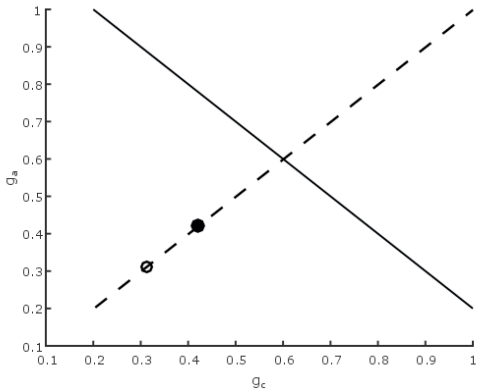

Figure 8: Summary of the results shown in Figure 7. Solid line represents a perfectly linear, additive model. Dashed line represents the points at which g_c is equal to g_a. The hollow point represents the mean of g_a g_c solutions in the posterior case that fell within five percent of the dashed line ($g_a = g_c = 0.312$). The filled point represents that same point for the anterior solutions ($g_a = g_c = 0.420$). These points were found to be significantly different ($p < 0.001$, bootstrap).

Discussion

In this study, we found that the medial giant axon taper and subsequent gradient in conduction velocity observed in *Lumbriculus variegatus* is also present in *Lumbricus terrestris.* In addition, we used a H-H computational model of an action potential to simulate nerve impulse conduction across the high fidelity gap junctions that join the roughly 100 interneurons of the medial giant fiber (Lyckman and Bittner, 1992). Using our model, we found that, while axonal conductance seems to be the primary predictor of conduction velocity, the strength of the gap junction coupling plays a significant role as well. Because axonal conductance was dependent upon axon diameter and the strength of gap junction coupling was not, these results make sense. The diameter of the axon not only affected the axonal conductance, but also the capacitance of the fiber. Thus, when analyzing the effects of g_a and g_c on conduction velocity, we found that g_a was the more significant contributor. This

difference between g_a and g_c lessens as conduction velocity increased. Mathematically, we can confirm this observation by considering how the capacitance changes as diameter increases.

At lower conduction velocities, axon diameter is relatively small, and at higher conduction velocities, axon diameter is larger. The dependence of capacitance on diameter is first-order and the dependence of axonal conductance is second-order. Thus, as diameter increases, g_a contributes more relative to capacitance in our model, whereas, at low conduction velocities, capacitance has a more significant impact. As the impact of capacitance lessens with increasing conduction velocity, g_c approaches equal contribution to g_a in our model.

The electrophysiological and histological data presented in this paper are consistent with previous work in *Lumbriculus variegatus* (Zoran and Drewes, 1987). Therefore, it seems likely that both the axon taper and decrease in conduction velocity are evolutionarily conserved traits. Based on computational results, this axon taper seems to significantly alter conduction velocity in the fibers from the anterior of the worm to the posterior. It seems that this taper is primarily responsible for this result. However, at higher conduction velocities (in the anterior of the worm) our computational model indicates that the strength of the gap junction coupling between interneurons plays an almost equal role in prediction of conduction velocity. This novel finding presents us with a unique look into the role of gap junctions in nerve impulse conduction and their interaction with anatomical axon properties, namely axon diameter. This information could potentially be useful in the study and treatment of demyelinating diseases where a full understanding of the biophysical properties underlying nerve impulse conduction is critical.

In order to confirm the results of the computational model more work needs to be done, particularly with physiology and pharmacology. To accomplish this, one would need to test the predictions that one: g_c plays a significant role in predicting conduction velocity, and two: that its contribution increases when axon diameter increases. In order to do this, one would have to record conduction velocity in the anterior and posterior of *Lumbriculus terrestris,* both in the presence of a gap junction antagonist and in the absence of a gap junction antagonist. Unfortunately, these gap junctions are very difficult to uncouple, making this experiment impossible until sufficient pharmacological and/or genetic tools become available.

Acknowledgements

We would like to thank Henry Schares and J.T. Paine for help in preliminary data collection.

Corresponding Author

Kevin Crisp
St. Olaf College
1520 St. Olaf Avenue
Northfield, MN
55057
crisp@stolaf.edu

References

Bullock TH (1945) Functional Organization of the Giant Fiber System of Lumbricus, Journal of Neurophysiology 8: 55-71.

Cole ES, Crumley AE, Carlson SM (2011) Patterns of sex determination in the scaly pearl oyster in four anchialine ponds on San Salvador Island, Bahamas, The 13th

Symposium on the Natural History of the Bahamas

Drewes CD, Landa KB, McFall JL (1978) Giant nerve-fiber activity in intact, freely moving earthworms, Journal of Experimental Biology 72: 217-227.

Guenther J (1973) Overlapping sensory fields of the giant fiber systems in the earthworm, Naturwissenschaften 60:521-522.

Hartline DK, Colman DR (2007) Rapid conduction and the evolution of giant axons and myelinated fibers, Current Biology 17: R29-R35.

Hodgkin AL, Huxley AF (1952) A quantitative description of membrane current and its application to conduction and excitation in nerve, J Physiol London 117: 500-44.

Kaldt N, Hanslik U, Heinzel HG (2010) Teaching basic neurophysiology using intact earthworms, Journal of Undergraduate Neuroscience Education (JUNE) 9:A20-A35.

Lyckman AW, Bittner GD (1992) Axonal conduction and electrical coupling in regenerating earthworm giant-axons, Experimental Neurology 117: 299-306.

Nelson P (1966) Comparaison Des Modeles De Neurone De Hodgkin-Huxley Et De Nelson, Bulletin of Mathematical Biophysics 28(3): 347-54.

NeuroDynamix: Computer-based neuronal models for neurophysiology W. Friesen - Jonathon Friesen - Oxford University Press - 1994

Principles of neuroscience Eric Kandel - Appleton & Lange - 2005

Shannon KM, Gage GJ, Jankovic A, Wilson JW, Marzullo TM (2014) Portable conduction velocity experiments using earthworms for the college and high school neuroscience teaching laboratory. Advances in Physiology Education 38: 62-70.

Zoran MJ, Drewes CD (1987) Rapid escape reflexes in aquatic oligochaetes: Variations in design and function of evolutionary conserved giant fiber systems, J. Compar. Physiol. 161:729-738.

Zoran MJ and Martinez VG (2009) Lumbriculus variegatus and the Need for Speed: A Model System for Rapid Escape, Regeneration, and Asexual Reproduction. In: Annelids in Modern Biology, pp 185–202. John Wiley and Sons.